D1.1.1 - Data set from Task 1.1 (object geometry, landscape structures)

IRTA

Dataset 1

During 2019 – 2021, several flights have been conducted in different orchards and vineyards with an unmanned aerial vehicle (UAV). In each flight, images were acquired with an UAV equipped with a multispectral (MACAW Tetracam or Micasense red-edge) + RGB camera (SONY alpha 6000) + Thermal camera (FLIR SC655). Only images from the multispectral and RGB have been used in this task. Image acquisition altitude varied from 50 to 70 m agl.

The objective is to use the spatial information collected to estimate the structural and biophysical parameters of the vegetation. For instance, object geometries such as crown area, canopy height, canopy volume, leaf area index (LAI), fraction of intercepted radiation (FIPAR) and fractional of green vegetation cover (FVC) are some of the parameters estimated using different approaches. The approaches vary between simple vegetation indices to 3D radiative transfer modelling.

The orchards and vineyard have different training systems, planting spacing distances and irrigation treatments. Also, concomitant to image acquisition in-situ data was collected related to the structural properties of the vegetation as well as leaf area index (LAI) and the fraction of intercepted radiation (FIPAR).

In addition to UAV flights, an almond orchard was also scanned in March and June 2021 with a terrestrial LIDAR. The objective is to also use this data for the same goal as with the UAV images, as well as to compare both approaches.

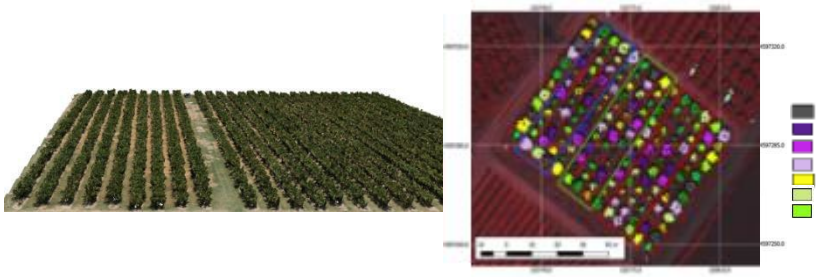

Fig. 1. Example of point cloud obtained with an UAV in the almond orchard.

Fig. 2. Photograph of the terrestrial LIDAR scanning the almond trees.

The dataset (Dataset 1) can be downloaded in the following link:

https://irtacat-my.sharepoint.com/:f:/g/personal/joaquim_bellvert_irta_cat/EkGG1qJDPAtFmNeOHMQzVrEBXcYQ4z06fOSDldmStErg5g?e=LnFnsO

The dataset consisted on UAV images collected in each field for the following dates:

Table 1. Dataset of image acquisition in different fields

Field/year	2019	2020	2021
Almond	03/07/2019		24/03/2021
	24/07/2019		19/05/2021
			03/06/2021
			29/06/2021
			29/07/2021
Vineyard		21/07/2020	21/06/2021
			08/07/2021
			18/07/2021
Apple			22/07/2021

For each date, there is the final orthomosaic as well as the Metashape Agisoft project file, which includes the different outputs (i.e. dense cloud, depth maps, model, point cloud, orthomosaic). Files with in-situ measurements (folders insitu_data) are also part of the dataset. LIDAR dataset is too heavy to be shared, but it is also available and can be shared in private using other procedures.

Publication: Bellvert Joaquim, Nieto Héctor, Pelechá Ana, Jofre-Čekalović Christian, Zazurca Lourdes, Miarnau Xavier. (2021) Remote Sensing Energy Balance Model for the Assessment of Crop Evapotranspiration and Water Status in an Almond Rootstock Collection. Frontiers in Plant Science. 12, nº608967.

Dataset 2

A study was set up to assess differences in biophysical variables and evapotranspiration of an almond orchard with three different planting systems. The almond orchard was planted in June of 2009 under three different production systems: open vase with a spacing distance of 5.5 x 3.5 m, central axis with 5 x 3 m, and hedgerow with 4.5 x 3 m (Fig. 1). Each production system was subjected to three different irrigation treatments: (i) Full-irrigation control, where irrigation aimed to meet ET requirements (100% ET_C) throughout the growing season, (ii) mild stress, irrigated at 50% ET_C throughout the growing season; and (iii) severe stress, irrigated at 20% ET_C throughout the growing season.

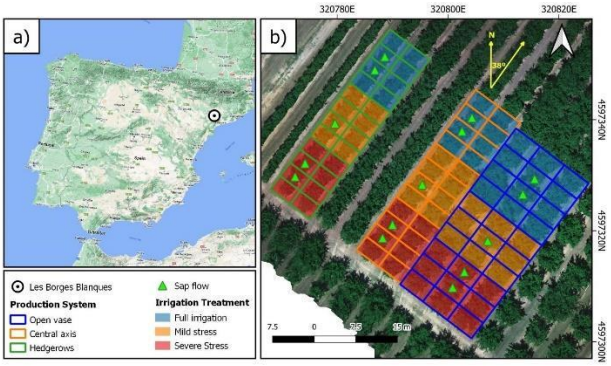

Fig. *3.* Location of the almond field in Les Borges Blanques (Lleida, Spain) (a) and experimental design of the field (b), showing in different colors the three production systems and the three irrigation treatments.

The image acquisition campaign consisted of five flights conducted on March 24, May 19, June 3 and 29, and July 29 of 2021. All flights were carried out with an UAV Dronehexa XL (DRONETOOLS, Seville, Spain) equipped with a multispectral and thermal camera.

To retrieve T_c and T_s separately and the biophysical traits, a canopy layer was obtained. The canopy layer was created based on a contextual classification using the DEM and the soil-adjusted vegetation index (SAVI). Pixels with a DEM greater than 1.5 m and SAVI greater than 0.2 were classified as canopy, while pixels that did not meet the conditions were classified as soil. The canopy layer was used to extract the T_c and T_s from thermal images, while T_{rad} corresponds to the total average temperature in each scene. The fractional canopy cover (f_c), canopy height (h_c) and canopy width (w_c) were obtained using the canopy layer and DEM. In addition, the canopy volume (v_c), normalized difference vegetation index

(NDVI), normalized difference water index (NDWI) and modified triangular vegetation index (MTVI2) were calculated as additional inputs of a machine learning approach for estimating LAI in all trees. According to Gao et al. (2022), who compared machine learning algorithms to estimate LAI, the random forest technique performed slightly better than the other algorithms. Therefore, the random forest algorithm was trained in this study to estimate LAI using the contextual, spectral, structural information as input data (production system, v_c, f_c, w_c, h_c and the canopy mean and canopy standard deviation of the vegetation indexes NDVI, NDWI and MTVI2) and the measured LAI as calibration data. Fig 2b shows the methodological scheme used to obtain the main parameters needed for the TSEB model.

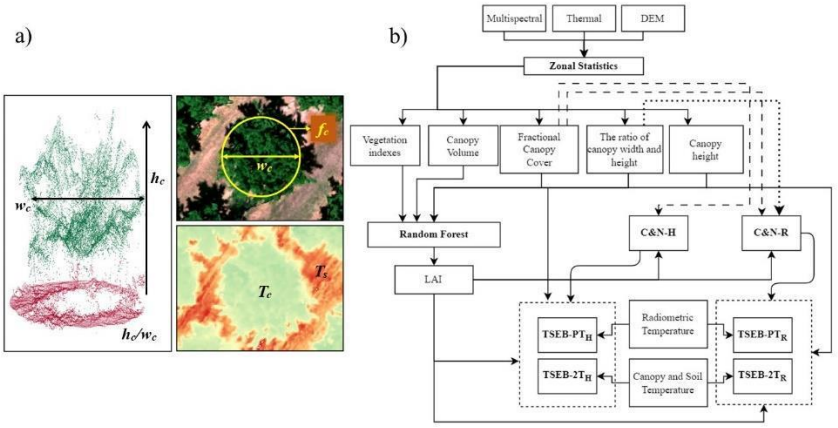

Fig. *4*. Flowchart of the procedures used for processing the multispectral and thermal images and the digital elevation model (DEM) in order to obtain the different biophysical variables of the vegetation and some of the inputs needed in the different two-source energy balance (TSEB) modelling approaches.

The dataset (Dataset 2) consists on all the inputs (TSEB_INPUTS_2021) needed for the TSEB modelling scheme and outputs (ENERGY_FLUXES) obtained from the TSEB, for each tree and image acquisition date. A metadata file is also available explaining the meaning of each variable.

https://irtacat-my.sharepoint.com/:f:/g/personal/joaquim_bellvert_irta_cat/EkGG1qJDPAtFmNeOHMQzVrEBXcYQ4z06fOSDldmStErg5g?e=LnFnsO

More information about the publication can be find here:

https://www.researchgate.net/publication/370075742_Assessment_of_transpiration_in_different_almond_production_systems_with_two-source_energy_balance_models_using_high_resolution_aerial_imagery

For more detail information about the dataset, orchard properties or other issues regarding dataset, please contact with: joaquim.bellvert@irta.cat.

CESBIO

"MetGen" is a stochastic weather generator that relies on low resolution reanalysis data to generate scenarios of meteorological variables at sub-daily temporal resolution. The stochastic weather generator is based on generalized linear models (GLM) for each meteorological variable with a suitable probability distribution (Normal, Gamma or Binomial). It's used to obtain a multi-site multi-variable surrogate series that fills the gaps in the observation period and extends it in the past. Several homogeneous stations within the region, in terms of climate - systematic variability - and weather - random variability -, may be used to calibrate the SWG. It models jointly several meteorological variables basing on strong inter-variable dependencies identified. Sub-daily resolution modelling is achieved by introducing covariates at the sub-daily resolution. Each meteorological variable is modelled by a regression model that is used stochastically for simulation according to its own probability distribution, whose parameters are driven by a large set of covariates. In addition to the low resolution meteorological variables provided by the reanalysis data (ERA5 here), other covariates are used to introduce inter-variable dependencies, deterministic effects (geographical information, seasonal and diurnal cycles) and memory effects, i.e. lagged values. The memory effects are computed either directly from the variable of interest, from spatial averages (the average of the values at all the sites at the given time step), from moving averages with a window of one day (48 steps of time) or less, or from a combination of a spatial and moving averages. These effects allow to take into consideration the past behavior of the variables. On another hand, the use of the large-scale reanalyses in the covariates of the GLM-based SWG is often quite helpful as it convey generally rather well the temporal dynamics of the at-site meteorological variables. Finally, additional covariates could be added for specific variables to improve the fit of the SWG.

Here, we propose a longterm “virtual meteorological station” for the Kairouan plain, from 2000 till now, based on ERA5 reanalysis and recent (2011-now) weather stations.

Publications:

2021 Farhani N., Carreau J., Kassouk Z., Mougenot, B., Le Page, M., Lili-Chabaane, Z., Zitouna-Chebbi, R., Boulet G., Regional sub-daily stochastic weather generator based on reanalyses for surface water stress estimation in central Tunisia, Environemental Modelling and Software, in revision.

2020 Farhani N., Carreau J., Boulet G., Kassouk Z., Mougenot B., Lepage M., Lili Chabaane Z., Zitouna R., Scenarios of Hydrometeorological Variables Based on Auxiliary Data for Water Stress Retrieval in Central Tunisia, 2020 Mediterranean and Middle-East Geoscience and Remote Sensing Symposium (M2GARSS), 2020, 293-296 (oral + proceeding)

Dataset available on https://osr-cesbio.ups-tlse.fr/

UNICA

During 2020 and 2021, several datasets have been collected in the Orroli study site.

Data collected consisted on the following:

- Geoelectrical measurements for the description of aquifer structure and definition of soil structure.
- Radar satellite data to assess soil moisture content
- Disaggregated climate model simulations using the Multivariate quantile mapping bias Correction for the Orroli site

The Geolectrical measurements consist of electrical resistivity tomography ERT along transect 9 transects in the Orroli site. The Geoelectrical database includes raw and processed data.

Radar satellite consist of two remote sensor products retrieved from the Sentinel satellite constellation. The first was the SAR mounted on Sentinel 1 to detect the dielectric constant of the surface soil, which is related to soil moisture, and the second was the multispectral optical radiometer mounted on Sentinel 2, to detect vegetation characteristics. The Sentinel 1 radar data were derived from S1A and S1B satellites, which carry a C-band synthetic-aperture radar instrument, and the level-1 Ground Range Detected GRD was used. The images were calibrated, corrected from the noise with a Lee filter 7 X 7, and resampled at a 30 m spatial resolution. From the backscatter signal of the radar ($^{o}_{vv}$) time series the soil moisture is estimated using a revised version of the Dubois model accounting for vegetation effects on radar signal

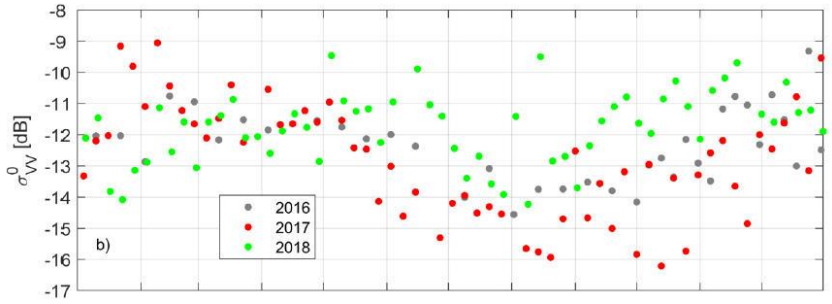

The remote sensing dataset includes the raw and processed data, and soil moisture estimates.

Dataset available on:

https://drive.google.com/drive/folders/1mDIb8WEQszEb1a2ASyZpg369UIyve8z_?usp=sharing

Publications:

Montaldo N, Fois L, Corona R. Soil Moisture Estimates in a Grass Field Using Sentinel-1 Radar Data and an Assimilation Approach. Remote Sensing. 2021 Jan;13(16):3293;https://doi.org/10.3390/rs13163293

Montaldo, N., Corona, R., Curreli, M., Sirigu, S., Piroddi, L. and Oren, R., 2021. Rock water as a key resource for patchy ecosystems on shallow soils: digging deep tree clumps subsidize surrounding surficial grass. Earth's Future, 9(2), p.e2020EF001870. https://doi.org/10.1029/2020EF001870

Contact person for datasets (Nicola Montaldo): nmontaldo@unica.it

INAT

Spatial variability in soil infiltrability

The objective was the monitoring of soil infiltration at the Merguellil watershed. After that a determination of Soil moisture will be done using of times series of optical and microwave remote sensing. We were interested in the upstream area of Merguellil watershed, located in Kairouan region (Figure). The mini disk infiltrometer was used for making field measurements. Fifty locations were chosen to monitor water soil infiltration (figure) based on soil types and Textural classes.

The methodology is based on the application of water on the soil surface through a porous disk at a constant negative pre-set pressure (figure).

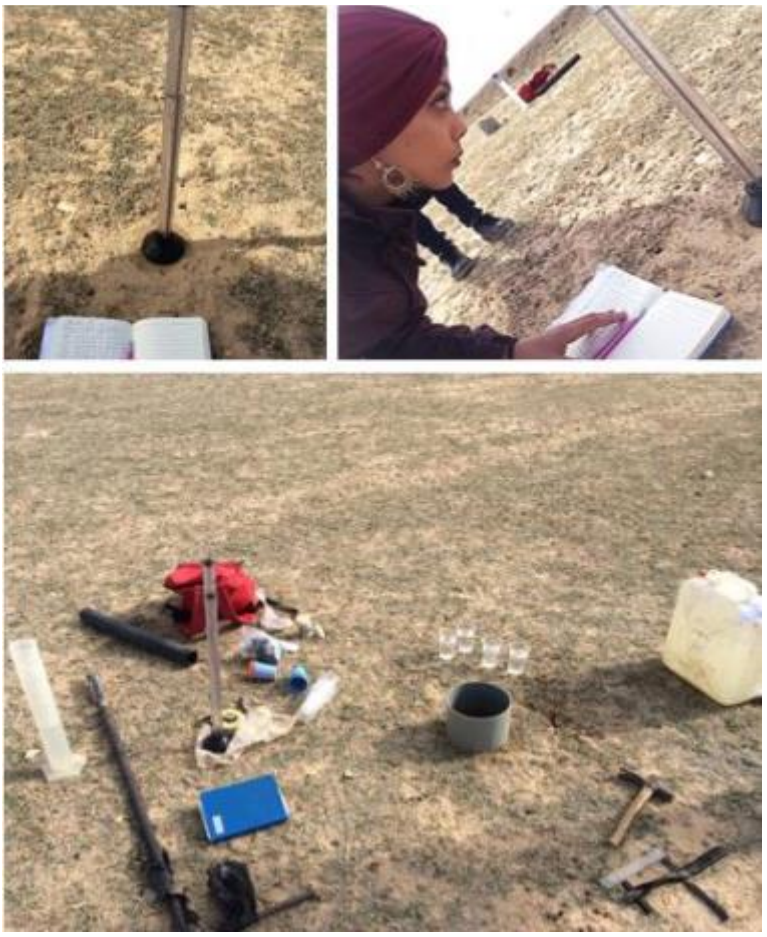

Figure 1 mini disk infiltrometer to measuer water infiltration at field

Results

mini disk infiltrometer | h1- 7 mm

grande base | 0.108

volume	temps	t [s]	temps global [s]	t [min]	différence de temps [s]	infiltration	racine²(t)	I/ racine²(t)
380	00:00:00:00	0	0	0	0		0	0
370	00:00:31:34	31.34	31.34	0.52	31.34	1.08	[illegible]	[illegible]
360	00:00:36:45	36.45	67.79	1.13	36.45	2.16	[illegible]	[illegible]
350	00:00:41:04	41.04	108.83	1.81	41.04	3.24	[illegible]	[illegible]
340	00:00:40:28	40.28	149.11	2.49	40.28	4.32	[illegible]	[illegible]
330	00:00:39:41	39.41	188.52	3.14	39.41	5.4	[illegible]	[illegible]
320	00:00:42:94	42.94	231.46	3.86	42.94	6.48	[illegible]	[illegible]
310	00:00:41:04	41.04	272.5	4.54	41.04	7.56	[illegible]	[illegible]
300	00:00:42:24	42.24	314.74	5.25	42.24	8.64	[illegible]	[illegible]
290	00:00:44:02	44.02	358.76	5.98	44.02	9.72	[illegible]	[illegible]
280	00:00:48:59	48.59	407.35	6.79	48.59	10.8	[illegible]	[illegible]
270	00:00:42:32	42.32	449.67	7.49	42.32	11.88	[illegible]	[illegible]
260	00:00:49:86	49.86	499.53	8.33	49.86	12.96	[illegible]	[illegible]
250	00:00:45:04	45.04	539.97	8.99	45.04	14.04	[illegible]	[illegible]
240	00:00:46:01	46.01	585.98	9.76	46.01	15.12	[illegible]	[illegible]
230	00:00:47:44	47.44	632.82	10.55	47.44	16.2	[illegible]	[illegible]
220	00:00:46:89	46.89	679.71	11.33	46.89	17.28	[illegible]	[illegible]
210	00:00:48:09	48.09	727.8	12.13	48.09	18.36	[illegible]	[illegible]
200	00:00:47:76	47.76	775.56	12.93	47.76	19.44	[illegible]	[illegible]
190	00:00:48:03	48.03	823.59	13.73	48.03	20.52	[illegible]	[illegible]
180	00:00:47:89	47.89	871.48	14.52	47.89	21.6	[illegible]	[illegible]
170	00:00:47:95	47.95	919.43	15.32	47.95	22.68	[illegible]	[illegible]

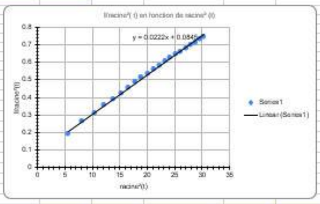

succion [mm]	θ	α	K [h]	Ks [mm/s]	Ks [mm/h]
-50	0.05	0.044537054840871	0.086457670	0.059866940	215.5210429
-70	0.02		0.002649916		

h2- 5 mm

volume	temps	t [s]	temps globale [s]	t [min]	différence de temps [s]	infiltration	racine²(t)	I/ racine²(t)
380	00:00:00:00	0	0	0			0	0
370	00:00:10:40	10.40	10.40	0.17	10.40	1.08	[illegible]	[illegible]
360	00:00:14:17	14.17	24.65	0.41	14.17	2.16	[illegible]	[illegible]
350	00:00:13:87	13.87	38.52	0.64	13.87	3.24	[illegible]	[illegible]
340	00:00:16:08	16.08	54.6	0.91	16.08	4.32	[illegible]	[illegible]
330	00:00:14:92	14.92	69.52	1.16	14.92	5.40	[illegible]	[illegible]
320	00:00:17:07	17.07	86.59	1.44	17.07	6.48	[illegible]	[illegible]
310	00:00:17:24	17.24	103.83	1.73	17.24	7.56	[illegible]	[illegible]
300	00:00:16:26	16.26	120.09	2.00	16.26	8.64	[illegible]	[illegible]
290	00:00:16:53	16.53	136.62	2.28	16.53	9.72	[illegible]	[illegible]
280	00:00:18:58	18.58	155.2	2.59	18.58	10.80	[illegible]	[illegible]
270	00:00:17:26	17.26	172.46	2.87	17.26	11.88	[illegible]	[illegible]
260	00:00:17:82	17.82	190.28	3.17	17.82	12.96	[illegible]	[illegible]
250	00:00:16:68	16.68	206.96	3.45	16.68	14.04	[illegible]	[illegible]
240	00:00:20:17	20.17	227.13	3.79	20.17	15.12	[illegible]	[illegible]
230	00:00:18:87	18.87	246	4.10	18.87	16.20	[illegible]	[illegible]
220	00:00:16:44	16.44	262.44	4.37	16.44	17.28	16.2	1.066666667
210	00:00:19:27	19.27	281.71	4.70	19.27	18.36	[illegible]	[illegible]
200	00:00:18:35	18.35	300.06	5.00	18.35	19.44	[illegible]	[illegible]
190	00:00:18:13	18.13	318.19	5.30	18.13	20.52	[illegible]	[illegible]
180	00:00:18:43	18.43	336.62	5.61	18.43	21.60	[illegible]	[illegible]
170	00:00:18:87	18.87	355.49	5.92	18.87	22.68	[illegible]	[illegible]
160	00:00:18:86	18.86	374.95	6.24	18.86	23.76	[illegible]	[illegible]
150	00:00:19:47	19.47	393.82	6.56	19.47	24.84	[illegible]	[illegible]
140	00:00:18:83	18.83	412.65	6.88	18.83	25.92	[illegible]	[illegible]
130	00:00:18:91	18.91	431.56	7.19	18.91	27.00	[illegible]	[illegible]
120	00:00:18:87	18.87	450.43	7.51	18.87	28.08	[illegible]	[illegible]

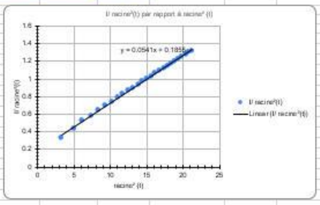

CERTE

-Characterization Aquifer Structure of Lebna dam (2019-2020): DATASET of geological, lithological and geophysical investigations, which included 67 vertical electrical soundings, 14 tomographies, 1 drilling well up to 30 m for calibration, and 6 piezometric surveys, were carried out.

- The data collection allowed the production of geologic maps, 3D resistivity diagrams, coastal aquifer piezometric maps (February and August 2020) as well as isobath maps of the aquifer.

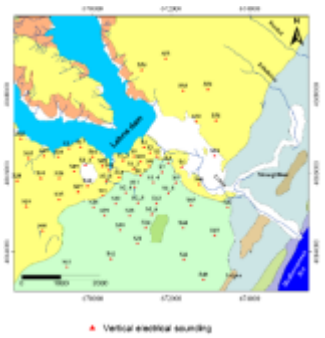

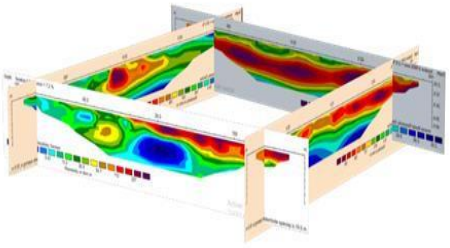

Contact person to share datasets: Fethi LACHAAL (lachaalfethi@yahoo.fr)

LISAH

Soil infiltration characteristics linked to soil surface characteristics (SSC) have been monitored over 34 fields in ORE OMERE, every two weeks during six years. Different climatic data, farmer practices and soil surface characteristics have been collected in different fields. Two different machine-learning approaches have been used to classify SSC types (single-date and multi-date), by using samples as 30/70 for test/training. Results suggested that both methods provided accurate performances (overall accuracy > 0.79) regardless of SSC to be investigated and of Sentinel-2 image to be used. The 'singledate' method did not allow the classification of SSC classes that were not observed at any date, while the 'multi-date' method allowed the classification of all SSC classes observed in the Sentinel-2 images. Future work will address the estimation of soil infiltrability from SSC.

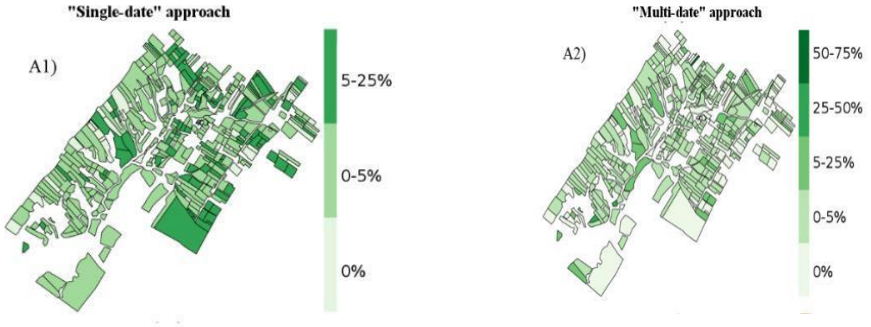

Publication:

Gomez C.; Sani A.M.; Lenco D.; Feurer D.; Jenhaoui Z.; Rafla A.; Teisseire M.; Baily J-S. (2022) Sentinel-2 images to assess soil Surface characteristics over a rainfed mediterranean cropping System. Catena, 231, 106152. https://doi.org/10.1016/j.catena.2022.106152

Contact person: Frederic Jacob (frederic.jacob@ird.fr) and Cécile Gomez (cecile.gomez@ird.fr)

UCAM

Clay content is an important parameter governing hydrodynamics properties of soils and consequently crucial to environmental management and agricultural development. The present study aims to use the textural middle infrared index (MID index) product of Landsat-8 Operational Land Images to map clay content over the Haouz plain (Central Morocco). The clay content was mapped at 30 m grid spatial resolution based on the relationship between the MID index and a large set of soil samples. Over the areas covered by green vegetation, the clay content was predicted using the ordinary cokriging technique. Then, this information was used to derive soil hydraulic properties such as the field capacity (θ_{fc}), the wilting point (θ_{wp}) and the saturated hydraulic conductivity (K_{sat}) by using different pedotransfer functions. The validation of the maps was performed by using independent soil samples and measurements. The results showed that the clay content is significantly correlated to MIDindex. The ordinary cokriging improved mapping of clay content over the Haouz plain (R^2 = 0.70, RMSE = 3.5%). The obtained maps of θ_{fc}, θ_{wp} and K_{sat} revealed a good correlation between the simulated values and the measured values.

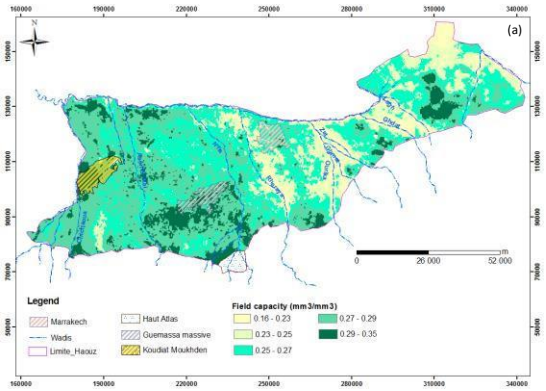

The spatial variation of moisture soil at Field capacity (θ_{fc}) over Haouz plain at 100 m spatial resolution

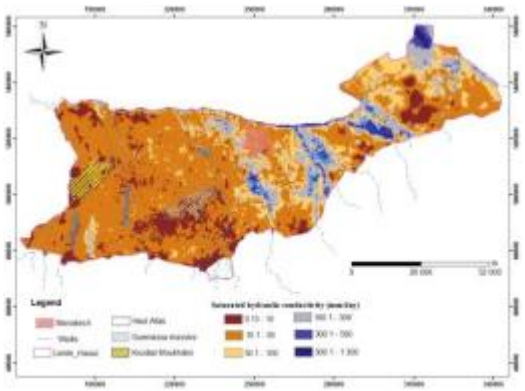

The spatial variation of saturated hydraulic conductivity (K_{sat})

Contact persons: Fakir Younes (fakir@uca.ac.ma)